Journal of Computer-Aided Molecular Design, **17:** 39–51, 2003.
KLUWER/ESCOM

Exploring the molecular basis of selectivity in A_1 adenosine receptors agonists: a case study

Fabrizio Giordanetto[a], Paola Fossa[b,*], Giulia Menozzi[b], Silvia Schenone[b], Francesco Bondavalli[b], Angelo Ranise[b] & Luisa Mosti[b]
[a]*Centre for Computational Science, Department of Chemistry, Queen Mary University of London, Mile End Road, London E1 4NS, United Kingdom;* [b]*Dipartimento di Scienze Farmaceutiche, Università degli Studi di Genova, Viale Benedetto XV, n.3 -16132 Genova, Italy*

Received 10 June 2002; accepted in revised form 12 December 2002

Key words: adenosine A_1 receptor, agonists, docking studies, homology modeling, 3D-model

Summary

Adenosine is a naturally occurring purine nucleoside that has a wide variety of well-documented regulatory functions and physiological roles. Selective activation of the adenosine A_1 receptor has drawn attention in drug discovery for the therapeutic effects on neural and cardiovascular disorders. We have developed a model of the human A_1 adenosine receptor using bovine rhodopsin as a template. A flexible docking approach has been subsequently carried out for evaluating the molecular interactions of twenty-one selective A_1 agonists with the receptor model. The results of these studies are consistent with mutational and biochemical data. In particular, they highlight a wide hydrogen-bonding network between the nucleoside portion of the ligands and the A_1 receptor as well as key amino acids for hydrophobic interactions with the different N^6-groups of the agonists. The models presented here provide a detailed molecular map for the selective stimulation of the adenosine A_1 receptor subtype and a steady basis for the rational design of new A_1 selective ligands.

Abbreviations: adenylate cyclase: AC, adenosine receptor: AR, G-protein-coupled receptors: GPCRs, transmembrane domain: TM

Introduction

Adenosine is essential for the proper functioning of every cell in the body, regulating many physiological processes, particularly in excitable tissues such as heart and brain. Its action derives from the activation of specific membrane receptors, generally referred to as purinoreceptors. Adenosine receptors (AR) have been intensively studied: to date four different adenosine receptor subtypes have been cloned in a variety of species, including humans [1]; these have been genetically and pharmacologically characterized as A_1, A_{2A}, A_{2B}, and A_3. All these receptors belong to the superfamily of the G-protein-coupled receptors (GPCRs), and contain an extracellular amino-terminal segment, seven transmembrane (TM) domains (α-helices) interconnected by six loops, and a cytoplasmic carboxy-terminal end [2].

Adenosine receptors exert their biological actions coupled to the intracellular enzyme adenylate cyclase (AC): A_1 and A_3 AR via G_i protein, while A_{2A} and A_{2B} via G_s protein, thus inhibiting or stimulating AC activity. In addition, coupling of ARs to other second messenger systems, such as calcium or potassium ion channels (A_1) or phospholipase C (A_1, A_{2B}, A_3) and D (A_3) have been described [3].

Adenosine receptors are ubiquitous. In particular, adenosine A_1 receptors are expressed in the central nervous system (CNS) and in internal organs such as heart, kidneys, liver and bladder. Due to this wide tissue distribution, the A_1 receptor subtype mediates a variety of biological effects. Consequently, A_1 regula-

*To whom correspondence should be addressed.
E-mail: fossap@unige.it

tion, through the aid of specific and selective ligands, could be of interest in the treatment of various central or peripheral pathologies. Adenosine A_1 receptor agonists may be useful in the treatment of hypertension, myocardial ischaemia, neurodegenerative disorders and peripheral neuropathy, whereas adenosine A_1 antagonists could serve as cognition enhancers, especially in alleviating the symptoms of Alzheimer's disease.

Up to now, various computer generated molecular models of ligand-AR complexes have been built and evaluated, one of the earliest being the bacteriorhodopsin-based model developed by Ijzerman [4], one of the latest the rhodopsin-based by Baraldi [5].

These models provided rational and structural guidelines for the design of adenosine receptor ligands. However, due to the ubiquitous character of the A_1 receptor subtype, no selective A_1 agonist is currently used in therapy and only a few A_1 antagonists have been approved as drugs [3, 6].

In the present work, with the aim of gaining a better understanding of the ligand-A_1 receptor interactions and in particular, to outline specific A_1 agonists binding mode, a theoretical model of the human A_1 receptor, developed by comparative modeling from the crystallographic structure of bovine rhodopsin [7], is presented. This model, refined on the basis of the actual knowledge derived from site-directed mutagenesis experiments, has been employed for extensive docking studies on a large set of A_1 agonists chosen from literature (Figure 1, Table 1) [8 and references cited therein] and on adenosine, the natural endogenous agonist of the receptor. This study suggests specific molecular interactions that can be shared by both the endogenous agonist and the synthetic agonists and others that are peculiar for the synthetic agonists only. The correct overlay of those interactions will provide a steady basis for rational design of new A_1 agonists.

Materials and methods

The amino acid sequences of the adenosine receptor family members were retrieved from the SWISSPROT database [9]. Multiple sequence alignment was performed alternatively employing CLUSTALW [10] and DIALIGN [11]. Amino acid conservation was calculated using phylogenetic relationship [12]. Secondary structure predictions were carried out using MEMSAT2 [13], PSIPRED V2.0 [14] and PREDICTPROTEIN [15]. Fold recognition and sequence to structure alignment was performed using THREADER [16]. The three-dimensional structure co-ordinate file of bovine rhodopsin [7] was obtained from the Protein Data Bank [17]. The three-dimensional models were generated by application of restraint-based homology modelling methods implemented in the program MODELLER [18]. Loop fragments were chosen according to the best score for homology and RMS fit for the anchor residues, as generated by loop search algorithms [19]. The final structure was subjected to 5000 steps of energy minimisation using the AMBER force field [20]. Subsequently, a 100 ps molecular dynamics simulation at 300° K (step length: 0.001 ps) involving only the side-chain atoms was carried out. The structure was then subjected to another 5000 steps of energy minimisation. Structural evaluation of the overall model was accomplished using the program PROCHECK [21].

The structural models of twenty-one A_1AR agonists collected from literature (Figure 1) have been docked to the adenosine A_1 receptor model with QXP [22]. The algorithm implemented in the QXP program allows for fully flexibility of the inhibitors and simultaneous flexibility of the active site side-chains. In this study, the side-chains of all the amino acids in the A_1 receptor model were allowed to move. Each docking run included 15000 steps of Monte Carlo perturbation, subsequent fast searching, and final energy minimisation. The results were evaluated in terms of total estimated binding energy, internal strain energy of the ligand, van der Waals and electrostatic interaction energies.

Results

The human adenosine A_1 receptor is a transmembrane protein consisting of 326 residues. The amino acid sequence of A_1AR appears to be very well aligned to the sequence of rhodopsin from *Bos Taurus* (Figure 2), for which a three-dimensional structure already exists [7]. Moreover, the secondary structure predictions for the A_1AR were found to be in good agreement with the structure assignments from bovine rhodopsin (Figure 2). The overall three-dimensional model of the A_1AR folds in an alpha bundle formed by 7 α-helices (A7-V36, A43-G72, Y76-V109, P121-G145, S176-L201, G227-F259 and S267-F291). The overall homology model built for the A_1AR is nearly identical to

Table 1. Protein–ligand interactions as displayed by the best docking orientation for each agonist.

Agonist	Interactions of the ribose ring	Interactions of the substituent at the 4′-position	Interactions of the adenine portion	Interactions of the N^6-substituent[a]
Adenosine	I95, H251, T277	H278	T91, Q92, I274	
2-Substituted derivatives				
CP-Isoguanosine	I95, H251, T277	H278	T91, Q92, I274, V187, W188	**V87, L88**
Doridosine	I95, H251, T277	H278	T91,Q92, I274, V187, W188, Y179	
BN-063	I95, H251, T277	H278	T91, Q92, I274, V187, W188, Y179	
AZ-1081	I95, H251, T277	H278	I274, N254	
CADO	I95, H251, T277	H278	T91, Q92, V187, W188, I274	
CCPA	I95, H251, T277	H278	T91, Q92, V187, W188, I274	**L88, Y179** V87, L88
NNC-210136	I95, H251, T277	H278	T91, Q92, V187, W188, I274	**L88, Y179** V87, L88, T270, Y271 Y12, Y271, F275
NNC-901515	I95, H251, T277	H278	T91, Q92, V187, W188, I274	**L88, Y179** V87, L88
NNC-210147	I95, H251, T277	H278	T91, Q92, V187, W188, I274	**L88, Y179** L88, Y179, F183, L258 Y12, V87, L88, Y271, F275
thio-CADO	I95	H278	Q92, V187, W188, N254, I274	
4′-Substituted derivatives				
NECA	I95, T277	I63, S94, H278	T91, Q92, I274	
RG-14202	I95, T277	I63, S94, H278	T91, Q92, I274	**L88**, **Y179** V87, L88
AMP-579	I95	I63, S94, H278	T91, Q92, W188	**V87, L88** Y12, T270, Y271, F275
UP202-32	T91	W247, L250, H251, T277	T91, Q92, W188	**Y12, T270, Y271, F275** Y12, V87, Y271
CPA	I95, H251, T277	H278	Q92, I274 V87, L88	**L88, Y179**
CHA	I95, H251, T277	H278	Q92, I274 V87, L88	**L88, Y179**
RG-14178	I95, H251, T277	H278	Q92, I274	**V87, L88, M180, F183, L258** V87, L88
R-PIA	I95, H251, T277	H278	Q92, I274	V87, L88 Y12, T270, Y271, F275
HPIA	I95, H251, T277	H278	Q92, I274	**Q92, L88, Y179** V87, L88
S-ENBA	I95, H251, T277	H278	Q92, I274	**L88, Y179** V87, L88
SDZ-WAG994	I95, T277		Q92, I274	**V87, L88**

[a]Bold style indicates the most favourable interactions. Subsequent lines indicate alternative interactions.

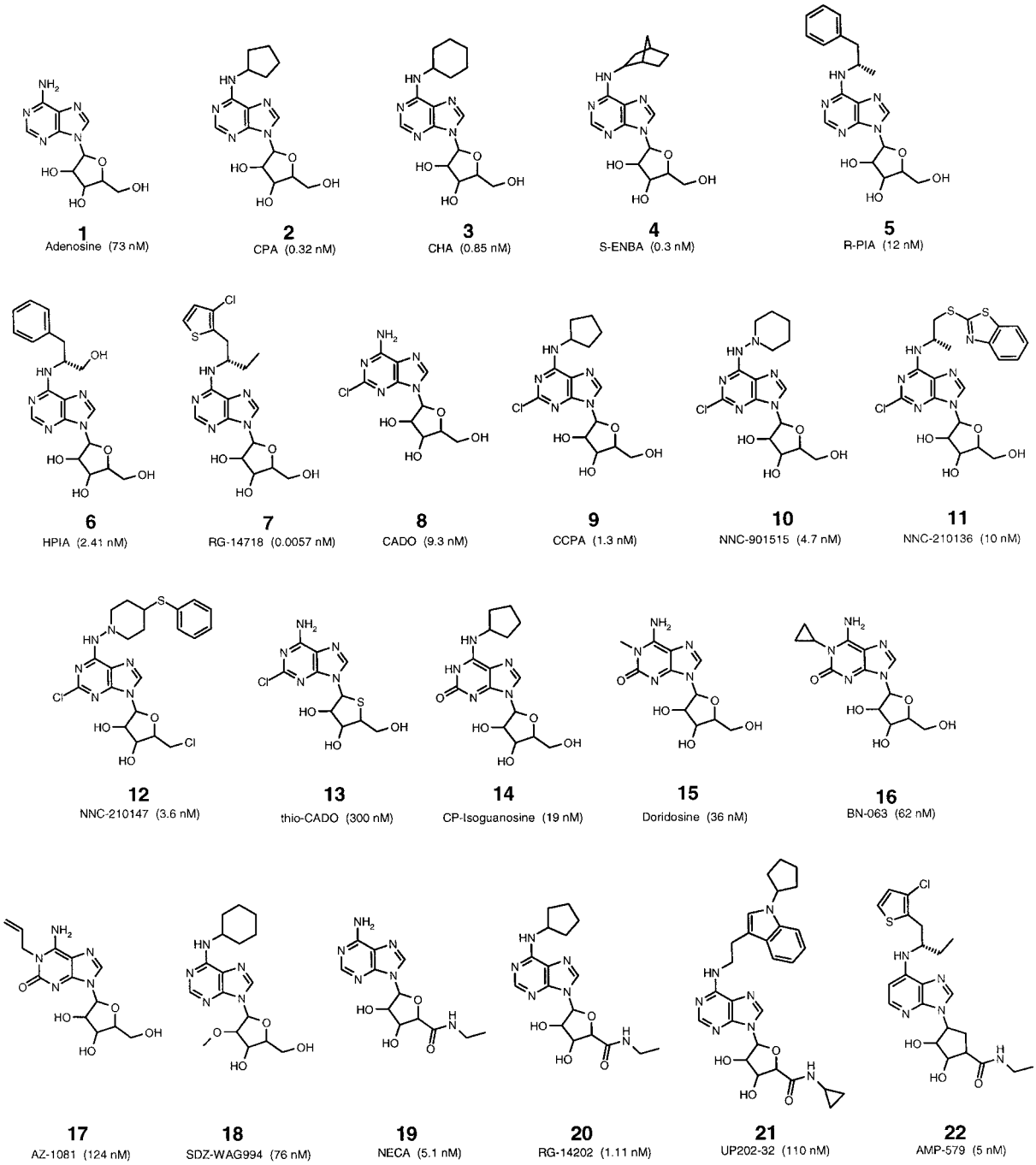

Figure 1. Molecular formulas of adenosine and selective A_1 agonists **2-22**. For each structure, Ki values determined on A_1 AR from rat brain membranes and expressed as nM, are reported in parenthesis [ref. 8 and literature cited therein].

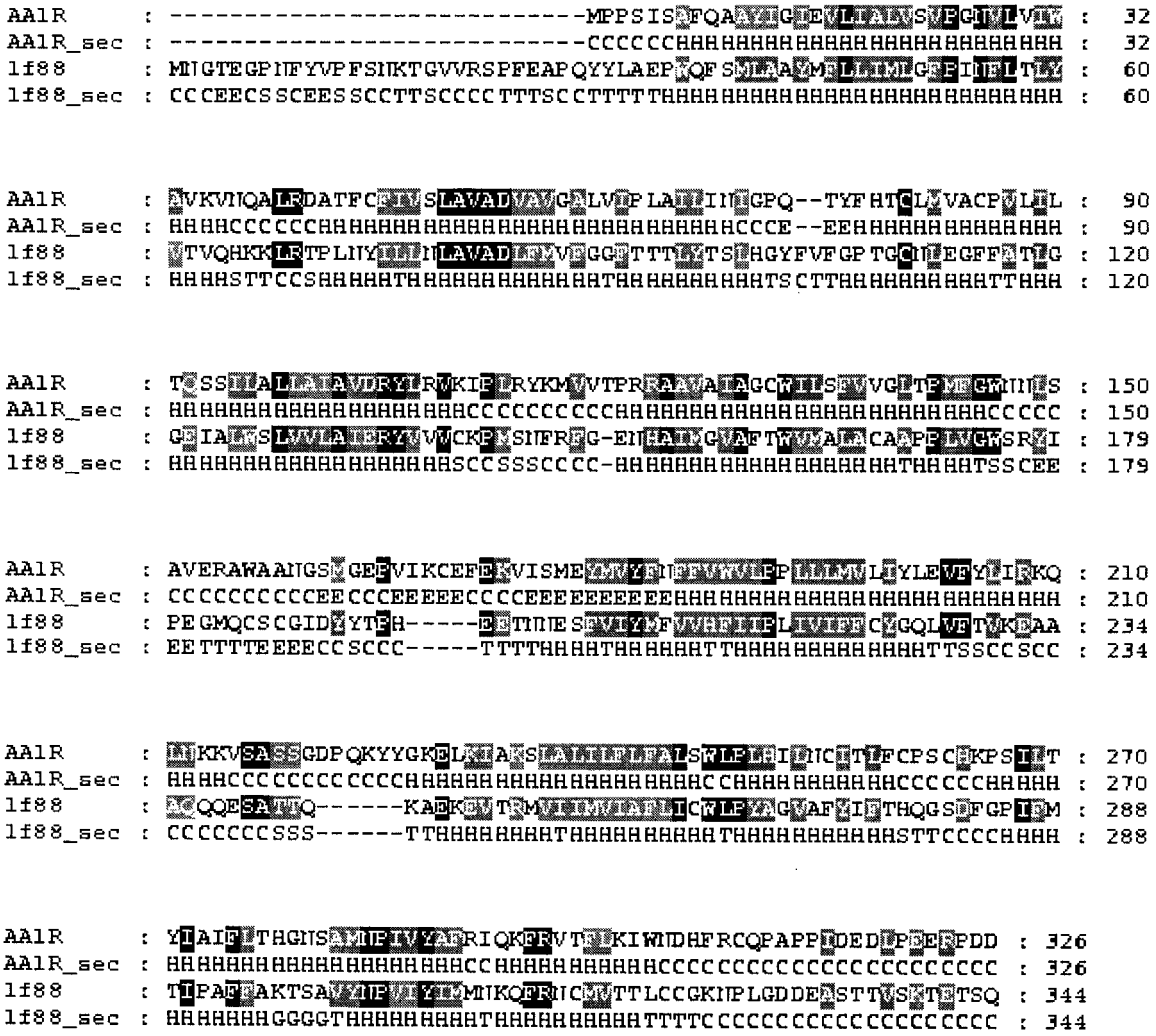

Figure 2. Sequence to structure alignment for the A_1A receptor. 1f88 is the PDB identifier for the three-dimensional structure of bovine rhodopsin [7]. Secondary structure predictions for the A_1AR are labelled accordingly (H: helix, C: coil). Secondary structure assignments for the template structure are indicated as follows. H: helix, E: extended strand, C: coil, B: isolated beta-bridge, G: 3/10 helix, S: bend, T: hydrogen bonded turn. Black shading indicates amino acid identities while grey shading represents conserved physico-chemical properties.

the three-dimensional structure of bovine rhodopsin, with a root mean square deviation of 0.263 Å using the alpha carbon atoms of the residues in the transmembrane helices.

Several site-directed mutagenesis studies have been performed on the A_1 receptor [23–26]. Substitutions of G14, E16, P25, P86, V88, T91, Q92, T277 and H278 have been found to affect the binding of ligands: in particular G14, E16, P25, P86 and T277 are specific for the agonist binding, while V88, Q92, T91 and H278 are involved also for the antagonist binding [27]. According to our model, G14, E16 and P25 are located on TM1, P86, V88, T91 and Q92 lie on TM3 whereas T277 and H278 reside on TM7. The central core of the alpha bundle is made up mainly by TM2, TM3, TM5, TM6 and TM7. TM1 interacts with TM2 and TM7 whilst TM4 packs against TM3 and TM5.

Adenosine and several synthetic agonists have been docked to the homology-built model of human A_1AR. Their chemical structures, as well as their potencies are given in Figure 1. The adenosine scaffold is a common structural feature of all the agonists. The main differences arise from chemical substitutions at the position 2 and 6 of the purine base and at 2′ and 4′ of the ribose ring. The computed molecular interac-

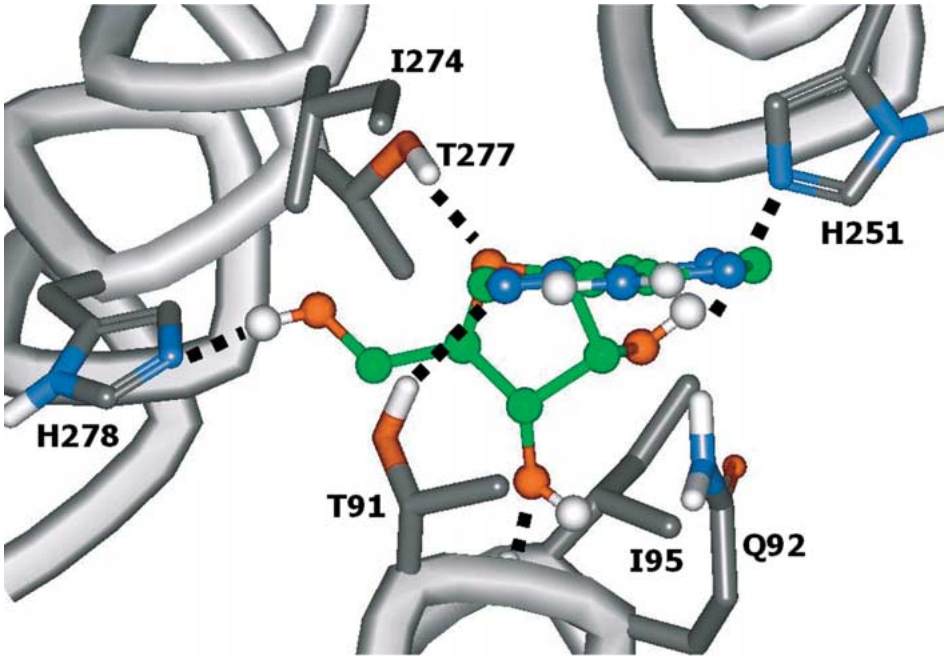

Figure 3. Proposed binding orientation for adenosine, A_1AR natural agonist.

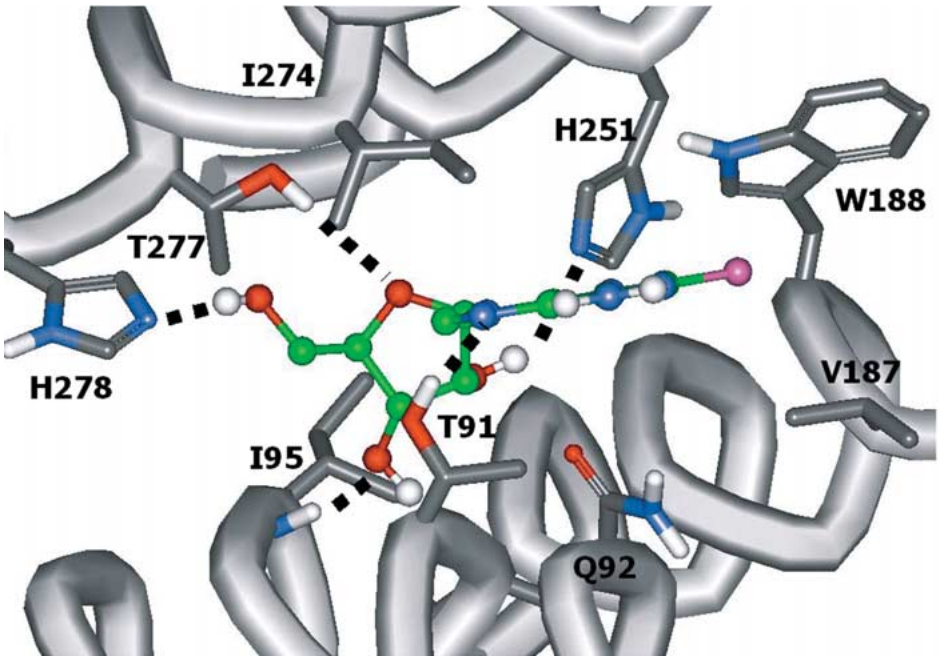

Figure 4. Docked model of CADO. The 2-Chlorine atom fits in a small cleft between V187 and W188 on TM5.

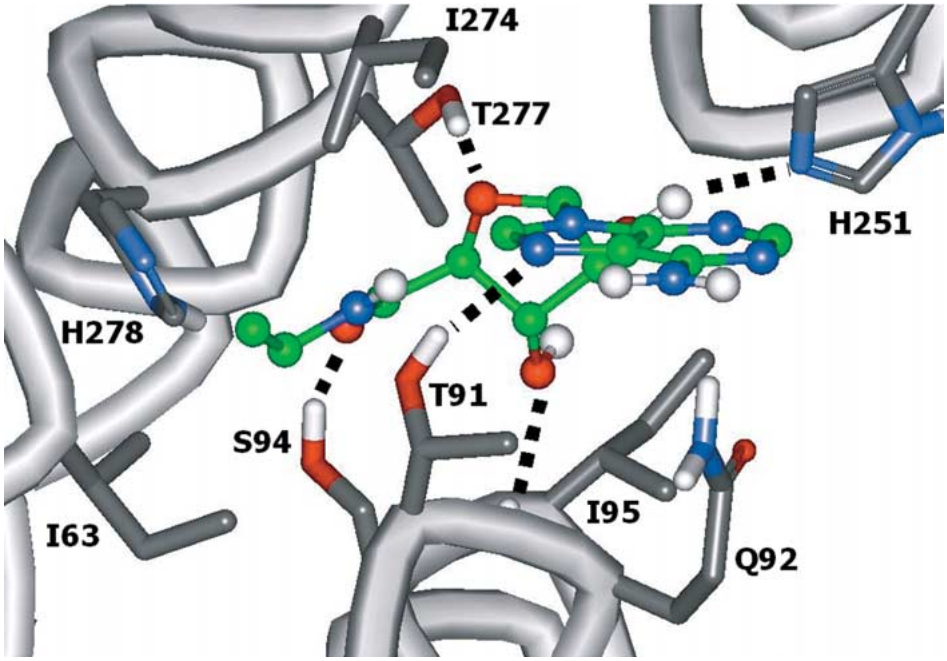

Figure 5. Predicted binding mode for NECA. The N-ethyl carboxamide function shows a H-bond with S94 and van der Waals contacts with I63 and H278.

tions for each ligand-receptor complex are displayed in Table 1.

The reduced availability of affinity data on A_1 agonists for the human A_1 receptor severely hampers the study of agonist-receptor interactions in the A_1AR model. We therefore employed a larger dataset of affinity values (expressed as K_i) as determined in rat brain [8 and references cited therein], considering that the sequences of the A_1AR in the two species have a percentage identity of 94.8% and the amino acid differences are located in the TM4-5 loop and in the carboxy-terminal cytoplasmic segment.

Adenosine

The docked model of adenosine (Figure 3) displays several polar interactions between the natural agonist and the receptor. N7 on the purine base is linked to T91 side-chain (TM3). The 2′OH, 3′OH and 5′OH groups are H-bonded to H251 imidazole ring (TM6), I95 backbone amide function (TM3) and H278 side-chain (TM7), respectively. Moreover, the ribose oxygen is engaged in a H-bond with T277 (TM7). The adenine ring is tightly packed against Q92 side-chain on TM3 and establishes additional van der Waals contacts with I274. The proposed model is consistent with site-directed mutagenesis data: T91, T277 and H278 in fact have been shown to be essential for the agonist binding [25]. Barbhaiya and co-workers[26] observed that mutation of S94 to alanine unpaired the binding of some A_1AR agonists. According to our docking results, the 5′OH group of adenosine and the other agonists could be involved in a H-bond with S94 instead of H278. However, our calculations display this alternative binding mode as energetically unfavourable when compared to 5′OH-H278, due to a higher energy state of the protein caused by the rearrangement of A_1AR S94 side-chain. This molecular rearrangement seems favourable only in the case of the N-ethyl-carboxamido substitution at position 4′ of the ribose ring (see below). Thus, our studies suggest that a 4′-hydroxy-ethyl group would establish a positive interaction with S94. Although mutation of S94 to alanine would impair a possible H-bond with the adenosine moiety of the agonists, we believe this is not enough to justify the loss of agonist binding, as witnessed by Barbhaiya [26], and we suggest that other mechanisms (i.e. alteration of the receptor conformation) could possibly be involved upon S94 substitution.

2- Substituted derivatives

Several agonists (CADO (**8**), CCPA (**9**), NNC-901515 (**10**), NNC-210136 (**11**), NNC-210147 (**12**) and Thio-CADO (**13**)) have a chlorine atom at position 2 of their adenine ring. The docked orientations of these ligands highlight that the halogen atom establishes extensive van der Waals contacts in a groove made up by the side-chains of V187 and W188 on TM5 (Figure 4). According to our calculations bromine atom would provide a better filling. The additional interactions observed here could justify the enhanced potency of CADO (**8**) (9.3 nM) with respect to adenosine (73 nM).

Other ligands (CP-Isoguanosine (**14**), Doridosine (**15**), BN-063 (**16**) and AZ-1081 (**17**)) show a carbonyl function at position 2. The carbonyl function points towards V187 and W188, similarly to the chlorine atom, whereas substituents at N1 point towards Y179 on TM5. Hydrogen, methyl and cyclopropyl can still be accommodated whereas the N1-allyl fragment of AZ-1081 (**17**) induces, interestingly, a different ligand orientation. By comparing the docking energies of Doridosine (**15**), BN-063 (**16**) and AZ-1081 (**17**) (−31.2 kJ; −28.0 kJ and −26.4 kJ respectively), our model suggests that larger substituents on N1 produce unfavourable contacts with the A_1 receptor and this trend seems to be confirmed by the decrease in affinity observed ranging from Doridosine (**15**) (36 nM) to BN-063 (**16**) (62 nM) and AZ-1081 (**17**) (124 nM).

4′-Carboxamide derivatives

NECA (**19**), RG-14202 (**20**), UP202-32 (**21**) and AMP-579 (**22**) possess a diversely substituted amide function at position 4′. In the case of the N-ethyl substitution, the amide carbonyl group displays a H-bond with the side-chain of S94 while the ethyl moiety is closely packed to I63 and H278 side-chains (Figure 5). S94 and H278 have been highlighted as essential for agonist binding by recent studies [25–26]. According to our results, these interactions replace the H-bond between the natural ribosylic OH in 5′ and the side-chain of H278 and could account for the increase in potency observed for NECA (**19**) (5.1 nM versus 73 nM of adenosine). If we compare RG-14178 (**7**) and AMP-579 (**22**) (0.0057 nM versus 5 nM), the replacement of the OH group in 5′ with the amide function seems to decrease the binding affinity in this case. However, additional structural changes that occur on the ribose part of AMP-579 (**22**) could be held responsible for the decreased affinity: according to our model, replacement of the ribose ring of RG-14178 (**7**) by a carbocyclic ring in AMP-579 (**22**) affects the molecular interactions displayed by the N^6-substitutent at the binding site, as described below. UP202-32 (**21**) is the only agonist with a N-cyclopropyl substitution on the amide function. The docked orientation displayed by UP202-32 (**22**) is completely different from the other 4′-carboxamide ligands. The cyclopropyl substituent protrudes towards a hydrophobic pocket (W247, L250, H251 and T277) between TM6 and TM7. The NH group of the amide function establishes a H-bond with H251 side-chain whereas N7 on the adenine ring retains a H-bond with T91. Due to the different rearrangement of the adenosine scaffold of UP202-32 (**22**), it displays only 2 polar interactions, compared to the five H-bonds displayed by the other carboxamide derivatives. These differences could be held responsible for the decreased affinity of UP202-32 (**22**) (110 nM).

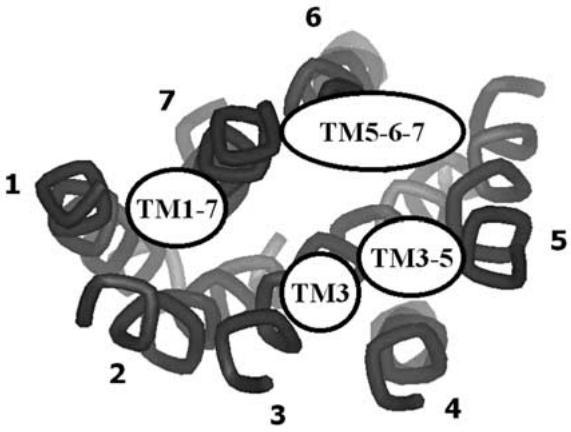

Figure 6. A_1AR lipophilic pockets available for the interaction with the different N^6-substituents.

Derivatives with other ribose modifications

A sulphur atom replaces the oxygen of the ribose moiety in thio-CADO (**13**). The resulting docked orientation is very dissimilar with respect to the one adopted by its close analogue CADO (**8**). The 4-thio-ribofuranosyl ring is shifted towards the upper part of the A_1AR core channel and the purine base is packed against N254 on TM6 and H274 on TM7. Compared to CADO (**8**), only two H-bonds are left. We could infer that the larger volume of the sulphur atom and its weaker H-bond acceptor character induce this less favourable pose and are probably responsible for the

difference in potency (300 nM of thio-CADO (**13**) versus 9.3 nM of CADO (**8**)). SDZ-WAG994 (**18**) (76 nM) differs from CHA (**3**) (0.85 nM) in that it is substituted with a methoxy group at 2′ on the ribose ring. According to the docking results, this chemical substitution impairs the H-bond with H251 and this could result in the decreased binding affinity.

N^6-substituted derivatives

The N^6 position is the most varied structural point of A_1AR agonists. For convenience in the discussion we shall divide the different N^6 groups into two classes. Set 'A' holds the simple rings (cyclopentyl, cyclohexyl, piperidin-1-yl and norborn-2-yl derivatives) whereas set 'B' contains the branched chains (1-(3-chloro-thiophen-2-ylmethyl)-propyl, 1-methyl-2-phenyl-ethyl, 2-(benzothiazol-2-ylsulfanyl)-1-methyl-ethyl, 3-phenyl-propan-1-ol). The physicochemical nature of the N^6-substituents is mainly hydrophobic. According to our models, several lipophilic pockets are available for a suitable interaction. These are depicted in Figure 6. TM3 is made up by V87 and L88; L88 and Y179 create TM3-5; TM5-6-7 consists of Y179, M180, F183 and L258 whilst TM1-7 is formed by Y12, T270, Y271 and F275.

The docking study shows that group A displays two possible interaction-modes. The first one places the N^6-substituents in the TM3 hydrophobic groove whereas the second binding mode inserts the N^6-groups in TM3-5 cleft. The importance of L88 for the binding of N^6-substituted agonists has already been pointed out by mutagenesis experiments [23]. The same study indicated that V87 is not essential for agonist binding. Addition of a cyclohexyl, cyclopentyl, and norborn-2-yl substituent at N^6 of adenosine leads to agonists with subnanomolar affinities. All the best-docked orientations for those ligands place the N^6-group closely packed to L88 and Y179. Our study suggests that the correct interaction with the TM3-5 pocket could be crucial for the agonist potency.

N^6-substituents belonging to group B show a larger conformational freedom. This is reflected by the different interaction modes displayed during the docking calculations. These can be clustered around three main hydrophobic pockets: TM1-7, TM3-5 and TM5-6-7. Substitution at adenosine N^6 position with 1-(3-Chloro-thiophen-2-ylmethyl)-propyl gives the best A_1AR agonist, RG-14718 (**7**), with a binding constant of 0.0057 nM. According to our results, the ethyl group is packed, similarly to the mode displayed by group A best ligands, on the TM3-5 pocket whereas the chlorothienyl moiety fits perfectly in the TM5-6-7 groove. This study reveals that the ethyl group of RG-14718 (**7**) mimics the first two methylenes of the group A substituents since they interact in the same way with the TM3-5 cleft (Figure 7). We could speculate that such a small fragment could be responsible for the correct complexation with L88 and Y179 on TM3-5 and could therefore justify the subnanomolar affinity of the compounds. This seems to be confirmed by K_i values of NNC-210136 (**11**) (10 nM) and R-PIA (**5**) (12 nM), both lacking a methyl on the N^6-group and unable to efficiently interact with TM3-5. Picomolar binding affinity values, on the other hand, would be the result of the additional interaction of the chlorothienyl fragment with the TM5-6-7 pocket. In this case, our results indicate that the chlorine atom on the thiophene ring is the responsible for the correct fit. The halogen atom, as correctly oriented by the thiophene ring establishes exhaustive van der Waals contacts with M180, F183 and L258. RG-14718 (**7**) is the only agonist that fills both TM3-5 and TM5-6-7 pockets. This co-operative mechanism could therefore be a target for new structure-based design projects.

Interestingly, AMP-579 (**22**) displays the same N^6 group but not with the same orientation. In the AMP-579 model, the N^6 substituent prefers to occupy the TM3 or alternatively the TM1-7 pocket. We believe this is due to the two additional molecular modifications: the replacement of oxygen by a methylene group and the substitution at 4′ position with an amide group. These structural differences result in a different orientation for the adenine moiety of the ligand, which in turn restrains the mobility of the N^6-substituent. This could account for the reduced affinity of AMP-579 (**22**) (5 nM) in comparison with RG-14718 (**7**).

HPIA (**6**) has a polar function on its N^6-substituent. Interestingly, this hydroxyl group can form a H-bond with Q92 on TM3. This interaction forces the remainder of the N^6-moiety to pack against the TM3-5 pocket. According to our model, chemical fragments longer than benzyl would be required to reach the TM5-6-7 cleft. Although HPIA (**6**) establishes an additional H-bond with Q92 when compared to RG-14178 (**7**), its N^6-substituent is not able to reach the TM5-6-7 hydrophobic pocket that, according to our calculations, is important for an optimal interaction with the A_1 receptor. Moreover, the van der Waals contact with V87 is also impaired for HPIA (**6**). This could help explain the difference in the binding affin-

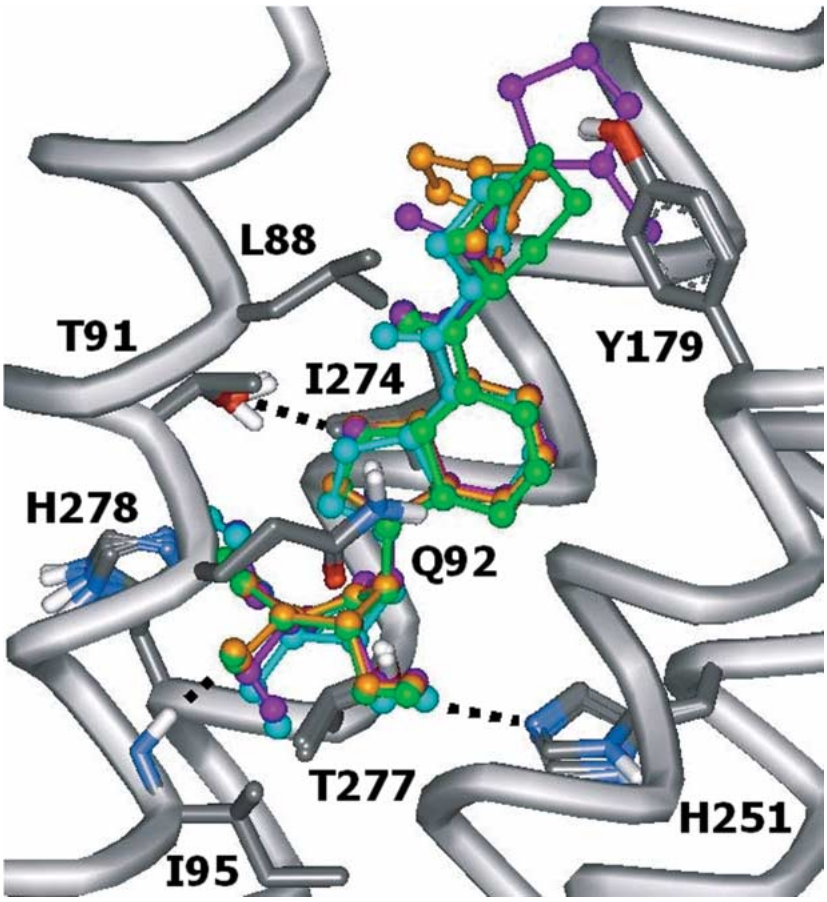

Figure 7. Superimposition of the docked poses of the best A_1AR agonists (purple: RG14718 (**8**), orange: S-ENBA (**8**), cyan: CPA (**8**), green: CHA (**8**)).

ity between HPIA (**6**) (2.41 nM) and RG-14178 (**7**) (5.7 pM).

Receptor subtypes selectivity

Figure 8 displays a multiple sequence alignment of the different human adenosine receptor subtypes. The A_1 receptor is closely related to the other isoforms with sequence percentage identities of 49.09%, 47.40% and 45.45% for the A_{2A}, the A_3 and the A_{2B} subtype, respectively. The transmembrane domains appear to be very well aligned with a strong conservation of the amino acids hydrophobicity. The larger amino acid variations occur within the intra- and extracellular loops and in the amino- and carboxy terminal segments.

The docking results indicate that the adenosine moiety of the A_1 ligands is involved in an extensive hydrogen-bonding network with T91, S94, I95, H251, T277 and H278 on the A_1 receptor. With the exception of H251 (replaced by a serine in the A_3 receptor) and T277 (substituted by a serine in the A_{2A}, A_{2B} and A_3 isoforms), all these amino acids are invariant throughout the different subtypes (Figure 8). However, the observed substitutions maintain the physico-chemical properties of the residues, therefore allowing H-bond interactions with the ligands. This is consistent with the fact that all AR subtypes need to recognise the natural agonist adenosine. An interesting mutation among the adenosine receptor isoforms occurs at position 63 of the A_1 receptor where a methionine occurs for the A_3 subtype. According to our models, I63 enjoys close packing with the N-ethyl group of the 4′-carboxamido-substituted agonists. It could therefore be possible to exploit the different conformational nature of these residues by precisely tailoring the 4′-substituent in order to achieve A_3 specificity.

Additional amino acid substitutions are located on TM5. Here the different AR subtypes can be divided

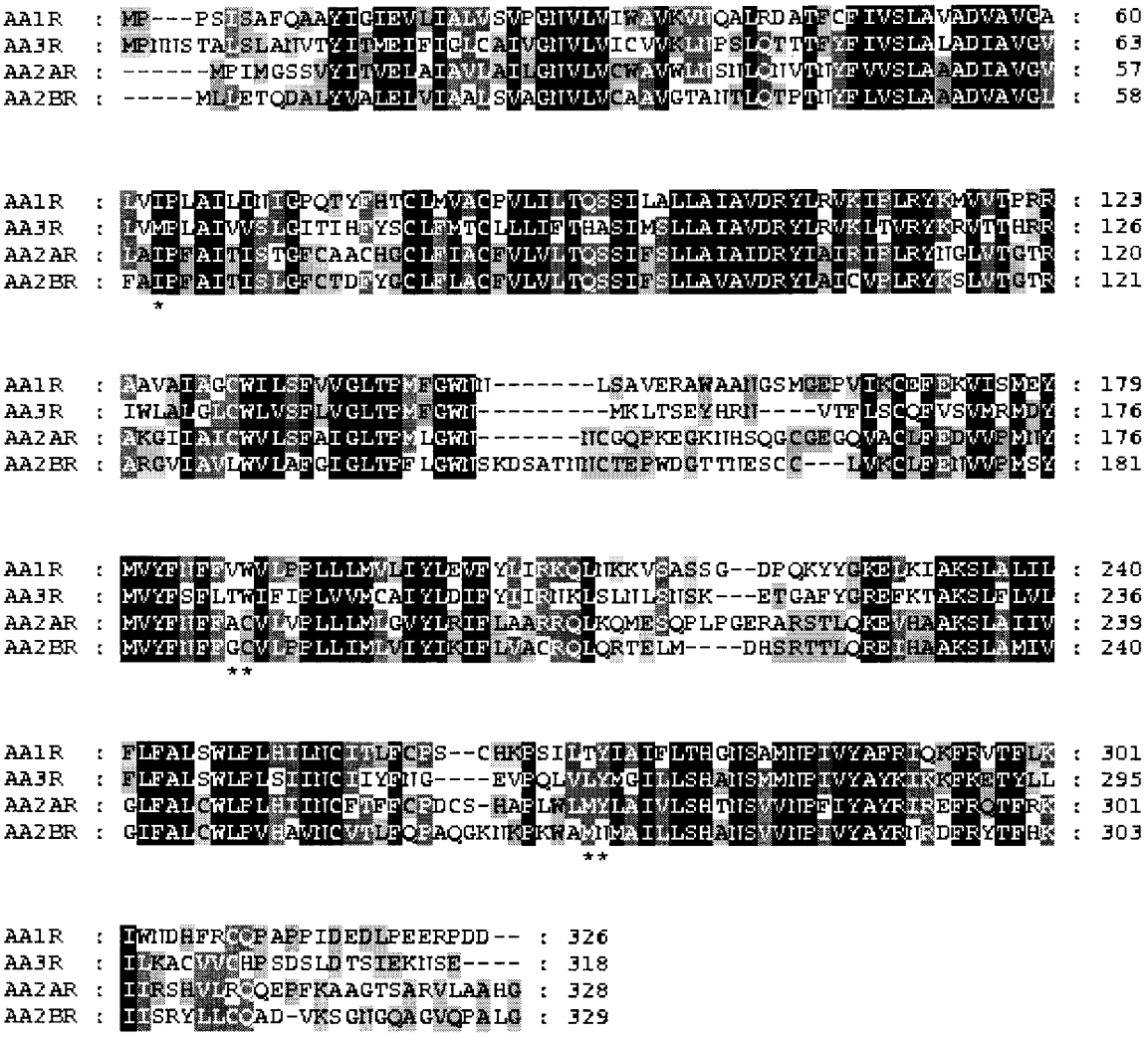

Figure 8. Multiple sequence alignment of the human adenosine receptor subtypes. Amino acid differences that can be exploited for selectivity are labelled with an asterisk. Colour shading: black, conserved percentage between 80 and 100; dark grey, between 60% and 80%, light grey, between 40% and 60%, white, less than 40%.

into two groups, according to the amino acids occurrence at position 187 and 188 of the A_1 isoform: A_1 and A_3 receptors (first group) show a β-branched (valine or threonine) and an aromatic (tryptophan) residue, A_{2A} and A_{2B} subtypes (second group) show a small residue (alanine or glycine) and a cysteine (Figure 8). According to the docking results, V187 and W188 are responsible for the complexation with the 2-substituent of the agonists (e.g. Chlorine substituent in CADO). The A_3 receptor is the only isoform displaying a polar residue (threonine). The side-chain volume of the two amino acids present on the $A_{2A/B}$ receptors is significantly smaller than the one on the A_1 and A_3 subtypes. This suggests that bulkier substituents at the 2-position could be much more tolerated in the A_2 subfamily than in the A_1 and A_3 isoforms. This structural discrimination could therefore be important in the quest for selectivity.

Different hydrophobic grooves are available for the interaction with N^6-groups in the adenosine A_1 receptor. The nature of these pockets appears to be overall conserved among the different receptor subtypes. However, interesting differences occur in the TM1-7 and in the TM5-6-7 clefts. T270 on the A_1 receptor is replaced by hydrophobic residues in the other isoforms whereas Y271 is substituted by an asparagine only on the A_{2B} subtype. Appropriate N^6-chemical

groups could thus target the polar character of these amino acids in an effort to increase specificity.

Conclusions

In an effort to better understand the molecular interactions between the human A_1AR and its agonists, we have developed a 3D-model of the receptor consistent with the available site-directed mutagenesis data, and we report on the binding mode of the natural endogenous agonist, adenosine, and of a large set of A_1 selective synthetic agonists. These models could be considered preliminary accounting for the different affinity data displayed from different agonists, as we do not provide at present a quantitative assessment of binding affinity differences. On the basis of our results we could confirm, for the synthetic agonists, the importance of interactions with amino acid residues L88, T91, I95, Y179, H251, I274, T277 and H278 previously highlighted by site-directed mutagenesis experiments. In addition, our model underlines the key role of substituents at position 2 and 6 of the purine base and at $2'$ and $4'$ of the ribose ring. According to our docking experiments, a chlorine atom seems to be the best substituent for position 2, while the optimal substituent on position 6 should be able to fit both TM3-5 and TM5-6-7 lipophilic pockets. Between the two, interaction with TM3-5 results essential for displaying low Ki values, while interaction with TM5-6-7 is not sufficient by itself but is however requested for further increasing the affinity. On the ribose ring, substitution of the ribose oxygen with a sulfur atom or a methylene group does not seem to improve affinity, determining the loss of an important interaction, *via* hydrogen bond, within the binding pocket. Similar considerations could be drawn for substitution on position $2'$ since the replacement of the hydroxylic group results detrimental for the interaction with residue H251. On position $4'$, substitution with a carboxamide group is acceptable if the substituent does not exceed the steric volume of an N-ethyl moiety, in all other cases it appears unfavourable.

Minor considerations concern substitution on position 1 in isoguanosine derivatives, where an hydrogen or a methyl group is tolerated but larger groups decrease affinity versus A_1 ARs.

In conclusion, although a structural homology derived model does not have the same degree of confidence of an experimentally determined one, the careful building procedure followed by us and the results obtained from the docking experiments indicate that our model is reliable enough to give helpful suggestions for the rational design of new potent agents with a specific mechanism of action and could be used for quantitatively exploring ligands' structure-activity relationship. Preliminary work has been done on this issue and some partial promising results have been obtained, however further investigations are already in progress and will be the future development of the present paper.

References

1. Dunwiddie, T.V., Masino, S., Annu. Rev. Neurosci., 24 (2001) 31.
2. Klotz, K.N., Naunyn-Schmiedeberg's Arch. Pharmacol., 362 (2000) 382.
3. Hess, S., Exp. Opin. Ther. Patents, 11 (2001) 1533.
4. IJzerman, A.P., van Galen, P.J.M., Jacobson, K.A., Drug Des. Discov., 9 (1992) 49.
5. Baraldi P.G., Cacciari B., Moro S., Spalluto G., Pastorin G., Da Ros T., Klotz K.N., Varani K., Gessi S., Borea P.A., J. Med. Chem., 45 (2002) 770.
6. Baraldi, P.G., Cacciari, B., Romagnoli, R., Spalluto, G., Exp. Opin. Ther. Patents, 9 (1999) 515.
7. Palczewski, K., Kumasaka, T., Hori, T., Behnke, C.A., Motoshima, H., Fox, B.A., Le Trong, I., Teller, D.C., Okada, T., Stenkamp, R.E., Yamamoto, M., Miyano, M., Science, 289 (2000) 739.
8. a) Muller, C.E., Curr. Med. Chemistry, 7 (2000) 1269; b) Knutsen, L.J.S., Lau, J., Petersen, H., Thomsen, C., Weis, J.U., Shalmi, M., Judge, M.E., Hansen, A.J., Sheardown, M.J., J. Med. Chem., 42 (1999) 3463.
9. Bairoch, A., Apweiler, R., Nucleic Acids Res., 28 (2000) 45.
10. Thompson, J.D., Higgins, D.G., Gibson, T.J., Nucleic Acids Res., 22 (1994) 4673.
11. Morgenstern, B., Frech, K., Dress, A., Werner, T., Bioinformatics, 14 (1998) 290.
12. Clamp, M., http://www.ebi.ac.uk/∼michele/jalview/, (1998).
13. Jones, D.T., Taylor, W.R., Thornton, J.M., Biochemistry, 33 (1994) 3038.
14. Jones, D.T., J. Mol. Biol., 287 (1999)797.
15. a) Rost, B. and Sander, C., J. Mol. Biol., 232 (1993), 584; b) Rost, B. and Sander C., Proteins, Struct. Funct. Genet., 19 (1994) 55; c) Rost, B., Sander, C., Schneider, R., *CABIOS,* 10 (1994) 53.
16. Jones, D.T., J. Mol. Biol. 292 (1999) 195.
17. Berman, H.M., Westbrook, J., Feng, Z., Gilliland, G., Beth, T.N., Weissig, H., Shindyalov, I.N., Bourne, P.E., Nucleic Acids Res., 28 (2000) 235.
18. Šali, A., Blundell, T.L., J. Mol. Biol., 234 (1993) 779.
19. a) Jones, T.A., Thirup, S., EMBO J., 5 (1986) 819; b) Claessens, M., Van Cutsem, E., Lasters, I., Wodak, S., Prot. Eng., 2 (1989) 335.
20. Pearlman, D.A., Case, D.A., Caldwell, J.W., Kollman, P., Comp. Phys. Comm., 91 (1995) 1.
21. Laskowski, R.A., MacArthur, M.W., Moss, D.S., Thornton, J.M., J. Appl. Cryst., 26 (1993) 283.
22. McMartin C., Bohacek R., J. Comput. Aided-Mol. Des., 11 (1997) 333.

23. Olah, M.E., Ren, H., Ostrowski, J., Jacobson, K.A., Stiles, G., J. Biol. Chem., 267 (1992) 10764.
24. Townsend-Nicholson, A., Schonfeld, P.R., J. Biol. Chem., 269 (1994) 2373.
25. Rivkees, S.A., Barbhaiya, H., Ijzerman, A.P., J. Biol. Chem., 274 (1999) 3617.
26. Barbhaiya, H., McClain, R., Ijzerman, A.P., Rivkees, S.A., Mol. Pharmacol., 50 (1996) 1635.
27. Fredholm, B.B., Ijzerman, A.P., Jacobson, K.A., Klota, K.-N., Linden J., Pharmacol. Rev., 53 (2001) 527.